J Electr Eng Technol.2015; 10(3): 1058-1065
http://dx.doi.org/10.5370/JEET.2015.10.3.1058

ISSN(Print) 1975-0102
ISSN(Online) 2093-7423

Current Dynamically Predicting Control of PMSM Targeting the Current Vectors

Hexu Sun, Kai Jing†, Yan Dong* and Yi Zheng***

Abstract – This paper present a current predicting control method for PMSM (permanent magnet synchronous motor) to improve the tracking performance of stator current, which regards the current vector as the control target. Solving the model state equation in the static frame (α-β frame), the dynamic change of current vector will be gained as three independent terms. These change terms, which contain the prediction of current vector, are discretized and simplified by Taylor series expansion and used to get the voltage vector as the predictive control quantity. SVPWM will transform the control voltage to the switching signal of inverter, which is newly deduced for the current vector. Simulation and experiment results are given to testy and verify the performance of this method.

Keywords: Current vector, Current tracking, PMSM, Dynamic predicting control.

1. Introduction

With the characteristics of high efficiency and high power density, PMSMs are applied in many high-performance servo systems in ordnance, industry and other fields. The electromagnetic torque of PMSM is a key to the performance of the servo systems, which is directly related to the control of stator current.

Predictive control is one method widely used in PMSM digital controller, just like model predictive control in [1] [2] and adaptive predictive control in [3], which is to predict the trend of motor states and give the optimum control amounts with the sampling values at current time so as to adjust the states accurately and in time. It is also effective for stator current control with higher performance of dynamic responding and tracking than the traditional hysteresis control and the digital PI control. Numerous studies have been done at home and abroad to pursue the superiorities of predictive control for stator current. [4-7] combine different predictive method to regulate the current for PMSM. In [4], current ripple has been identified for getting the rate of current changing; [5] has designed a feed-forward controller with best tracking algorithm; a robust predict control has been gained in [6] utilizing a discrete current equation and introducing a weighting factor; [7] expounds a current deadbeat control with Luenberger observer. These researches emphasize the development of predictive method for current control, but ignore the nature of current change. Moreover, the stator current is decomposed in the rotating frame (d-q frame) of rotor and the researches in [8] and [9] expect to control the two components independently by decoupling calculation. In [10], current PI control has only been developed by increase an integral prediction action in parallel for the current component of q-axis. It is complex for calculation in the frame which cannot directly reflect the dynamic change of the motor current vector.

This paper studies the motor current as the vector in static frame (α-β frame), where the dynamic change of the vector will be analyzed. The current vector predictive control will also be derived on discrete time. In section 2, the dynamic response of stator current vector about the sampling / control time will be gained from the current equation by Taylor series approximation. Section 3 will give the predictive control through the dynamic change of the current vector, and the SVPWM will also be newly deduced by the current vector and the voltage vector in the section. The simulations and experiments in section 4 will test and verify the performance of the proposed method.

2. Current Vector Dynamic Response and the Prediction

2.1 Dynamic response of current vector

Generally, the "voltage-current" equation of PMSM on d-q frame is expressed as follow:

$$\begin{bmatrix} u_d \\ u_q \end{bmatrix} = \begin{bmatrix} R_s + L_d p & -\omega L_q \\ \omega L_d & R_s + L_q p \end{bmatrix} \begin{bmatrix} i_d \\ i_q \end{bmatrix} + \begin{bmatrix} 0 \\ \omega \psi_f \end{bmatrix} \tag{1}$$

Where R_s represents the stator resistant, L_d, L_q the stator

† Corresponding Author: School of Control Science and Engineering, Hebei University of Technology, Co-constructing Labs with Central Enterprises, Tianjin, China. (jingkai_1082@ 126.com)
* School of Control Science and Engineering, Hebei University of Technology, Co-constructing Labs with Central Enterprises, Tianjin, China. (dongyan73@hebut.edu.cn, stephen_ claus@163.com)
** Hebei University of Science and Technology, Shijiazhuang, China. / School of Control Science and Engineering, Hebei University of Technology, Co-constructing Labs with Central Enterprises, Tianjin, China. (hxsun@hebust.edu.cn)
Received: October 3, 2014; Accepted: January 22, 2015

inductance on d and q-axis, u_d, u_q the d, q components of stator voltage, i_d, i_q the d,q components of stator current, ψ_f the rotor flux, ω the electrical angular velocity and p the differential operator.

The inductance L_d and L_q are equal for non-salient-pole PMSMs, which are written as L_s. Transform the equation above form the rotation d-q frame to the static α-β frame, of which the α-axis coincides with the normal direction of the A-phase winder, then the state space expression on the stator current components i_α, i_β will be rewritten as follow:

$$\begin{bmatrix} \frac{di_\alpha}{dt} \\ \frac{di_\beta}{dt} \end{bmatrix} = \begin{bmatrix} -\frac{R_s}{L_s} & 0 \\ 0 & -\frac{R_s}{L_s} \end{bmatrix} \begin{bmatrix} i_\alpha \\ i_\beta \end{bmatrix} + \frac{1}{L_s} \begin{bmatrix} u_\alpha \\ u_\beta \end{bmatrix} - \frac{\omega\psi_f}{L_s} \begin{bmatrix} -\sin\theta \\ \cos\theta \end{bmatrix} \quad (2)$$

where u_α, u_β are the α, β components of stator voltage, θ the electrical angle of rotor flux with respect to α-axis. Some assumptions are made for solving the dynamic response of stator current that the dynamic process is form t_0 and go through a very short time t, in which the speed ω can be considered constant and the position of the rotor $\theta = \theta_0 + \omega t$ that θ_0 is the initial position. Here, the input voltage $[u_\alpha, u_\beta]^T$ will also be considered as constants in the short time. So the general solution of the state space expression will be got as follow:

$$\boldsymbol{i}_s(t_0+t) = \boldsymbol{F}(t)\boldsymbol{i}_s(t_0) + \boldsymbol{G}(t)\boldsymbol{u}_s(t_0) + \boldsymbol{H}(t_0,t) \quad (3)$$

where $\boldsymbol{F}(t) = e^{-t/\tau}\boldsymbol{I}_{2\times2}$, $\boldsymbol{G}(t) = \frac{1}{R_s}(1-e^{-t/\tau})\boldsymbol{I}_{2\times2}$,

$$\boldsymbol{H}(t_0,t) = \frac{\omega\psi_f}{\sqrt{R_s^2+\omega^2 L_s^2}} \boldsymbol{Tr}\left(\theta_0 - \frac{\pi}{2} - \gamma\right) \begin{bmatrix} \cos\omega t - e^{-t/\tau} \\ \sin\omega t \end{bmatrix}$$

And $\tau = L_s/R_s$ is the time constant of PMSM, $\gamma = \arctan\frac{\omega L_s}{R_s}$ is an acute angel, $\boldsymbol{Tr}(\cdot)$ represent a rotation transformation written as matrix form $\begin{bmatrix} \cos(\cdot) & -\sin(\cdot) \\ \sin(\cdot) & \cos(\cdot) \end{bmatrix}$. If calculate the change of current vector, we get:

$$\begin{aligned} \Delta\boldsymbol{i}_s &\triangleq \boldsymbol{i}_s(t_0+t) - \boldsymbol{i}_s(t_0) \\ &= \underbrace{[\boldsymbol{F}(t)-\boldsymbol{I}]\boldsymbol{i}_s(t_0)}_{\Delta i_{si}} + \underbrace{\boldsymbol{G}(t)\boldsymbol{u}_s(t_0)}_{\Delta i_{su}} + \underbrace{\boldsymbol{H}(t_0,t)}_{\Delta i_{s\omega}} \end{aligned} \quad (4)$$

This formula consists of three independent terms, which are the change of zero input response $\Delta\boldsymbol{i}_{si}$, voltage input response $\Delta\boldsymbol{i}_{su}$ and emf response $\Delta\boldsymbol{i}_{s\omega}$ that are only determined by initial current vector $\boldsymbol{i}_s(t_0)$, control voltage vector and electrical angular velocity ω respectively.

2.2 Simplification and current prediction

Discretize the equation above from continuous domain with synchronous control/sampling cycle T_s that the interval $[t_0, t_0+t)$ can be mapped to the discrete cycle $[kT_s, (k+1)T_s)$. Within a cycle, all the terms are approximated by Taylor Series expansion and rewritten as "Amplitude-angle" form, we get:

$$\begin{cases} \left|\Delta\tilde{\boldsymbol{i}}_{si}(k+1|k)\right| = \frac{T_s}{\tau}\left|\boldsymbol{i}_s(k)\right| \\ \angle\Delta\tilde{\boldsymbol{i}}_{si}(k+1|k) = \angle -\boldsymbol{i}_s(k) \end{cases} \quad (5)$$

$$\begin{cases} \left|\Delta\tilde{\boldsymbol{i}}_{su}(k+1|k)\right| = \frac{T_s}{\tau}\frac{\left|\boldsymbol{u}_s(k)\right|}{R_s} \\ \angle\Delta\tilde{\boldsymbol{i}}_{su}(k+1|k) = \angle\boldsymbol{u}_s(k) \end{cases} \quad (6)$$

$$\begin{cases} \left|\Delta\tilde{\boldsymbol{i}}_{s\omega}(k+1|k)\right| = \frac{\psi_f\omega}{R_s}\frac{T_s}{\tau}\left(1-\frac{T_s}{2\tau}\right) \\ \angle\Delta\tilde{\boldsymbol{i}}_{s\omega}(k+1|k) = -\frac{\pi}{2} + \theta_k + \frac{1}{2}\omega T_s \end{cases} \quad (7)$$

And the terminal value of the current vector of the cycle can be expressed by these change terms and the initial value:

$$\begin{aligned} \hat{\boldsymbol{i}}_s(k+1|k) &= \boldsymbol{i}_s(k) + \Delta\boldsymbol{i}_s(k) \\ &= \boldsymbol{i}_s(k) + \Delta\tilde{\boldsymbol{i}}_{si}(k+1|k) + \Delta\tilde{\boldsymbol{i}}_{su}(k+1|k) + \Delta\tilde{\boldsymbol{i}}_{s\omega}(k+1|k) \end{aligned} \quad (8)$$

The dynamic change process depicted above is graphically expressed in Fig. 1, which is also a prediction of k+1 time from k time.

Resulting from the truncation error of Taylor series, the approximation errors of the current vector change terms are shown as follow by relative distance d_r:

$$d_{ri,u} = \frac{\left|\Delta\tilde{\boldsymbol{i}}_{si,u} - \Delta\boldsymbol{i}_{si,u}\right|}{\left|\Delta\boldsymbol{i}_{si,u}\right|} < \frac{1}{2}\frac{T_s}{\tau} + \frac{1}{12}\frac{T_s^2}{\tau^2} \quad (9)$$

$$d_{r\omega} = \frac{\left|\Delta\tilde{\boldsymbol{i}}_{s\omega} - \Delta\boldsymbol{i}_{s\omega}\right|}{\left|\Delta\boldsymbol{i}_{s\omega}\right|} < \frac{T_s^2}{24\tau^2}\sqrt{\left(\omega^2\tau^2-4\right)^2+1} \quad (10)$$

For the commonly used motor, the parameters meet $T_s/\tau \le 10^{-1}$, $\omega T_s \le 1$, so the relative distance $d_{ri,u}$<5.09%, $d_{r\omega}$ < 4.17%, which can guarantee the calculation error in

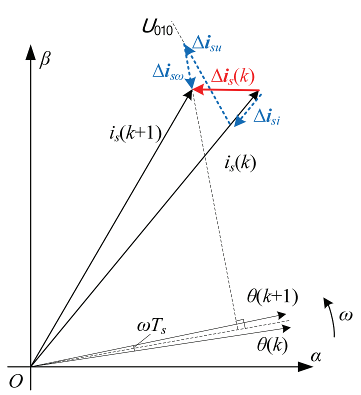

Fig. 1. Dynamic change of current vector

an allowable range.

Moreover, the results above will be affected by the uncertainty of motor parameters, for which these parameters, L_s, R_s as well as ψ_f, can be identified by recursive least square method with forgetting factor in [11].

3. Predicting Control for Current Vector

The typical current control timing sequence for discrete control system of PMSM is shown in Fig. 2(a): use the variables of k-1 time to deduce the control quantities which will be given to the motor system at k time, and the control result will be gained at the next sampling time (k+1). [12] point out there is two-cycle delay for the current tracking at least. However, current predictive control can shorten the delay (the sequence is shown in Fig. 2(b)), which regulates the current through the predictive value of k time by that of k-1 time that the delay reduces to one cycle.

The control quantity for [k, k+1) should be gained in the interval [k-1, k) and exported from k time. Substitute the predictive current of k time into that of k+1 time according to formula (8) and solve $\Delta\tilde{\boldsymbol{i}}_{su}(k+1|k)$, the control voltage $\boldsymbol{u}_s(k)$ will be given:

$$\begin{aligned}\boldsymbol{u}_s(k)=&\frac{\tau}{T_s}R_s\left[\boldsymbol{i}_s^*(k+1)-\boldsymbol{i}_s(k-1)\right]\\&+2R_s\boldsymbol{i}_s(k-1)-\boldsymbol{u}_s(k-1)-2\boldsymbol{u}_{s\omega}\end{aligned} \tag{11}$$

where $\boldsymbol{u}_{s\omega}=\frac{\tau}{2T_s}R_s\left[\left(1-\frac{T_s}{\tau}\right)\Delta\tilde{\boldsymbol{i}}_{s\omega}(k|k-1)+\Delta\tilde{\boldsymbol{i}}_{s\omega}(k+1|k)\right]$.

The $\boldsymbol{u}_{s\omega}$ can be simplified when the speed is considered constant in two adjacent cycles and expressed as "amplitude-angle" form:

$$\begin{cases}|\boldsymbol{u}_{s\omega}|\approx\psi_f\omega\left(1-\frac{T_s}{\tau}\right)\\ \angle\boldsymbol{u}_{s\omega}\approx-\frac{\pi}{2}+\theta_k+\omega T_s\end{cases} \tag{12}$$

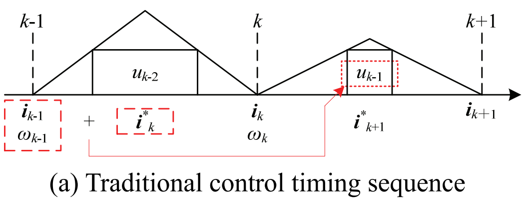

(a) Traditional control timing sequence

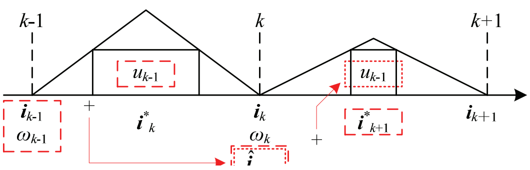

(b) Predicting control timing sequence

Fig. 2. Control timing sequence

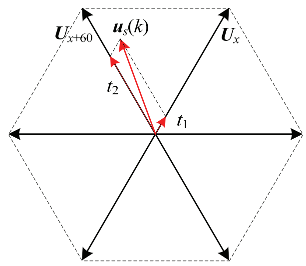

Fig. 3. Space voltage vector and the synthesis

SVPWM (space vector PWM)[13][14] is a modulation method that transforms the given voltage vector $\boldsymbol{u}_s(k)$ to the switch signal of inverter by matching the action time of the six effective voltage vectors and two zero voltage vectors, which shown in Fig. 3.

The traditional description of SVPWM is always about the synthesis of stator flux, but the action for stator current control is also a concern. in a control cycle, assuming that the action time of two adjacent effective voltage vectors $\boldsymbol{U}_x$ and $\boldsymbol{U}_{x+60}$ are t_1 and t_2 respectively which meet $t_1 + t_2 \le T_s$, and in the rest time the zero voltage vector $\boldsymbol{U}_0$ is export, the current change term $\Delta\boldsymbol{i}_{su}$ in formula (4) can be expressed as follow according to the superposition principle:

$$\begin{aligned}\Delta\boldsymbol{i}_{su}&=\boldsymbol{G}(t_1)\boldsymbol{U}_x+\boldsymbol{G}(t_2)\boldsymbol{U}_{x+60}+\boldsymbol{G}(T_s-t_1-t_2)\boldsymbol{U}_0\\&=\frac{1}{R_s}(1-e^{-t_1/\tau})\boldsymbol{U}_x+\frac{1}{R_s}(1-e^{-t_2/\tau})\boldsymbol{U}_{x+60}\end{aligned} \tag{13}$$

Simplify the formula as (6) and substitute the amplitude $2/3U_{dc}$ of voltage vector into it, the $\boldsymbol{u}_s(k)$ will be gained:

$$\boldsymbol{u}_s(k)=\frac{2}{3}\frac{U_{dc}}{T_s}\left(t_1\boldsymbol{e}_x+t_2\boldsymbol{e}_{x+60}\right) \tag{14}$$

where $\boldsymbol{e}_x$ and $\boldsymbol{e}_{x+60}$ represent the unit vector of $\boldsymbol{U}_x$ and $\boldsymbol{U}_{x+60}$. This formula also reflects the interrelation between voltage vector and current vector.

Then the predictive control quantity $\boldsymbol{u}_s(k)$ in (11) will be deduced as the switching time of three-phase inverter by (14), and the $\boldsymbol{u}_s(k$-1) also can use the calculated control quantity in the last cycle. Moreover, if the given voltage $\boldsymbol{u}_s(k)$ goes beyond the dashed hexagon in Fig. 3 that $t_1 + t_2 > T_s$, the action time will be reduced proportionally. The actual action time is represented as:

$$T_{1,2}=\begin{cases}\frac{T_s}{t_1+t_2}t_{1,2}, & t_1+t_2>T_s\\ t_{1,2}, & t_1+t_2\le T_s\end{cases} \tag{15}$$

4. Validation of Simulations and Experiments

4.1 Conditions for validation

We will select an M205B PMSM of KOLLMONGEN as

Table 1. Parameters of a PMSM

Parameters	Value	Parameters	Value
Max phase voltage(V)	250	Rate power(kW)	1.6
Rate current(A)	5.3	Rate torque(N·m)	4.47
Max current(A)	17.2	Max torque(N·m)	13.8
Rate speed(r/min)	3600	Pole pairs	2
Inductance(mH)	38	Rotor Flux(Wb)	0.2445
Resistance (Ω)	2.48		

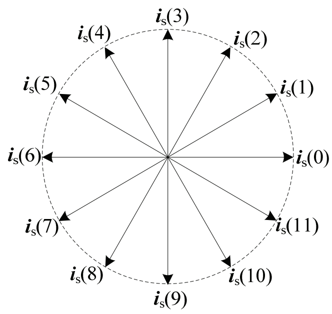

Fig. 4. 12 discrete current vectors

the motor for validation and its main parameters are listed in Table 1.

Here the control method of PMSM does not adopt the commonly used vector control but AC stepping control in [15], of which the given current is of discrete sine wave that the corresponding current vectors are discrete distributed in α-β frame. In the simulation the given current vectors are shown in Fig. 4 that the 12 uniformly distributed vectors in a cycle of electrical angle are given to current controller counterclockwise in turn.

The other conditions of the simulation include that DC bus voltage is 311V, switching frequency of inverter 10 kHz, Synchronous sampling cycle 100μs and the magnitude of the current vector 5A.

4.2 Simulation results of one step tracking

Fig. 5(a) shows the current dynamic change of A-phase when given vector varies from $\boldsymbol{i}_s(2)$ to $\boldsymbol{i}_s(3)$, in which the given current drawn in green jumped from 4.33A to 2.5A at 0.2001s and the actual current responded to this change at the next cycle and stably tracked the given after 7 cycles (the blue line); the red points are the sampling points. Fig. 5 (b) shows the dynamic process of the endpoint of actual current vector that varied from the initial position of 30° to 60° which is correspond to the given.

4.3 Simulation results of continuous running

The motor control strategy by discrete current vector has been studied for PMSM in [16] and [17], which utilize the angle difference between the discrete vector and the rotor position to generate a reposition torque and drive the rotor or implement positioning. The performance requirement of stator current control is higher for this control strategy, since the current vector is the key to the driving or reposition torque. Currently, the studies above used the method of DCC short for Direct Current Control in [18], which controls the current from the PMSM model in α-β frame, but omitting the effects of speed and the dynamic responses from current vector view. The comparison simulation of the proposed method and the DCC will be done as follow, which will use the method of "constant frequency control" that the switching frequency of current vector is a constant written as f_{const}. Here, the synchronous speed of the motor n and the fundamental frequency of the stator current f_i are determined by f_{const}, which meet $n = 2.5f_{const}$ for the PMSM with two pole pairs and $f_i = f_{const} / 12$.

Given f_{const} = 1Hz, 12Hz and 100Hz, and the motor speed n = 2.5r/min, 30r/min and 250r/min correspondingly. The stator current waveforms of the two current control methods are shown in Fig. 6, and the trajectories of the current vector endpoint are in Fig. 7.

In Fig. 6, the top three figures (a), (b) and (c) show the three-phase current waveforms of the proposed method, and the bottom three (d), (e) and (f) of DCC method. When f_{const} = 1Hz, the operation of the PMSM is not continuous but stepping. In each step, the rotor accelerated, decelerated, and stopped with a little oscillation. The simulation current waveforms are in (a) and (d) controlled by the two method respectively, which are similar at this low frequency. When f_{const} = 12Hz, the motor run continuously in a low speed when driving an inertial load. The current waveforms in (b) and (e) follow the given with little difference, but there are some spikes at each current

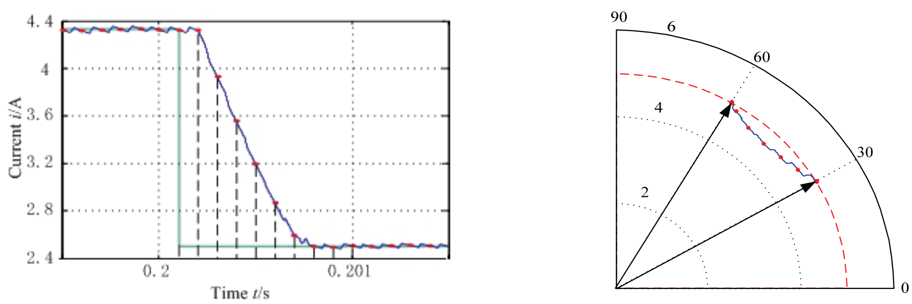

(a) Current tracking of A-phase

(b) Current vector tracking

Fig. 5. Dynamic tracking of the current vector

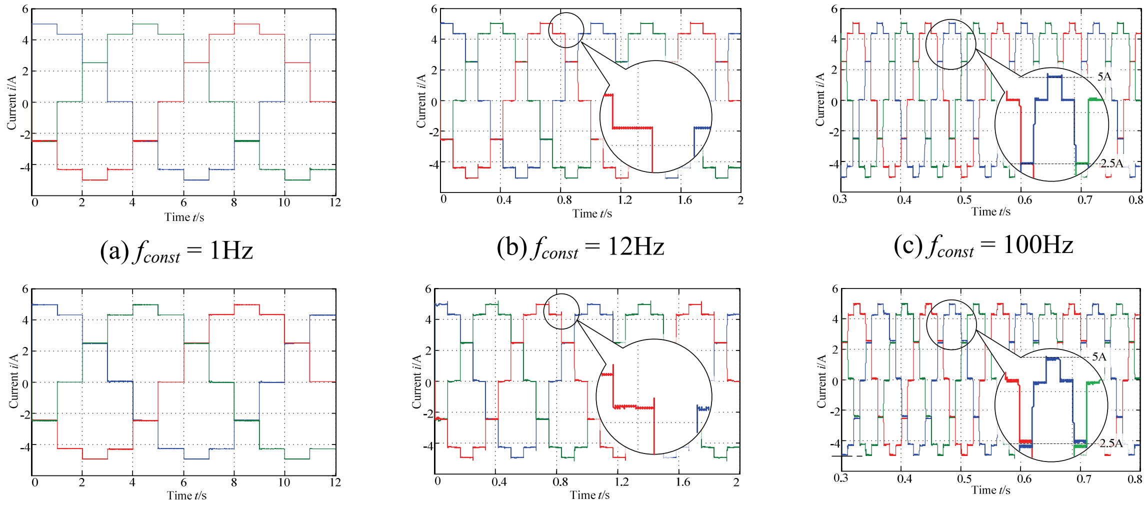

(a) f_{const} = 1Hz (b) f_{const} = 12Hz (c) f_{const} = 100Hz

(d) f_{const} = 1Hz (e) f_{const} = 12Hz (f) f_{const} = 100Hz

Fig. 6. Comparison of three-phase current waveforms in different frequencies

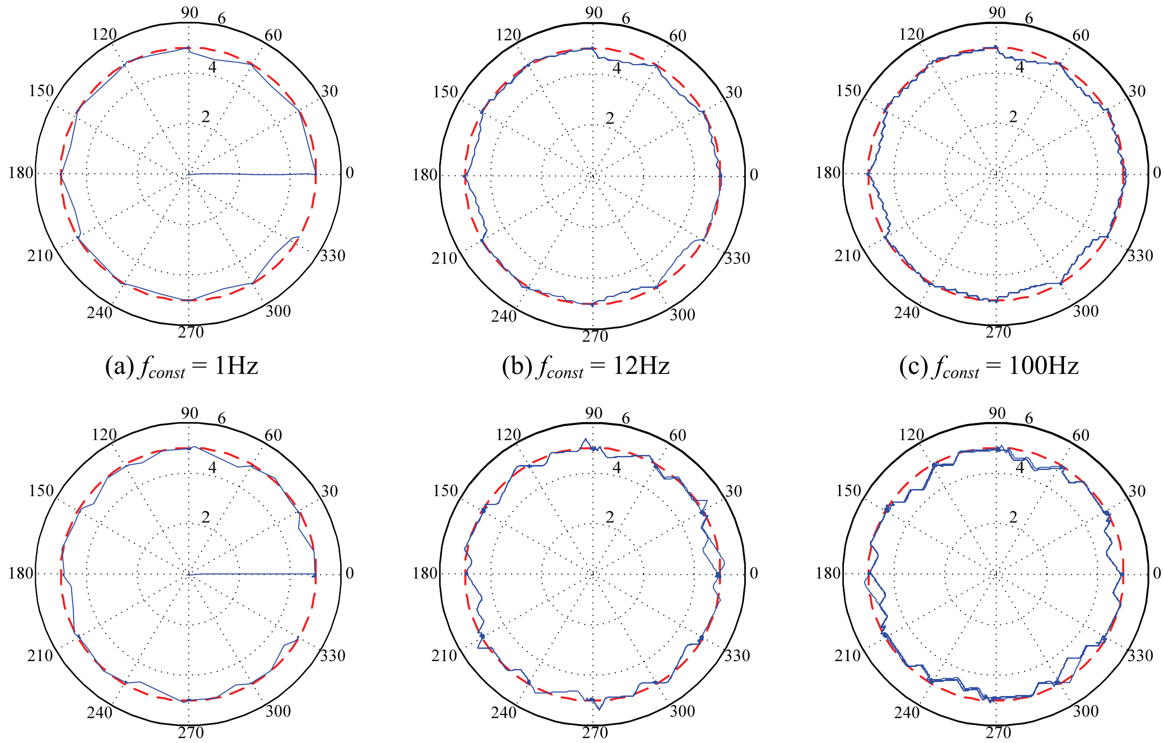

(a) f_{const} = 1Hz (b) f_{const} = 12Hz (c) f_{const} = 100Hz

(d) f_{const} = 1Hz (e) f_{const} = 12Hz (f) f_{const} = 100Hz

Fig. 7. Comparison of current vector endpoint trajectory in different frequencies

switching time in (e) of DCC method, which were enlarged in the circle and compared with the same part in (b). The last group (c) and (f) shows the waveform of 100Hz switching frequency, in which the same part of the waveforms were enlarged in the circle. In (f), the current tracking error appeared and the oscillation increased. Just like the part in the circle, the peak of the blue line could not reach the given value 5A and the tracking errors of the three phases are obvious at the value of 2.5A. However, these phenomena do not exist in (c) controlled by the proposed method.

Fig. 7 shows the control results from the view of vector, which is corresponding to them in Fig. 6 respectively. (The dashed reference circle is with radius of 5A) The figure (a), (b) and (c) resulted by the proposed method show the accurate tracking at the 12 discrete points and the smooth transition. The results of DCC method in (d), (e) and (f) are not so good to the former. When f_{const} = 1Hz, the result

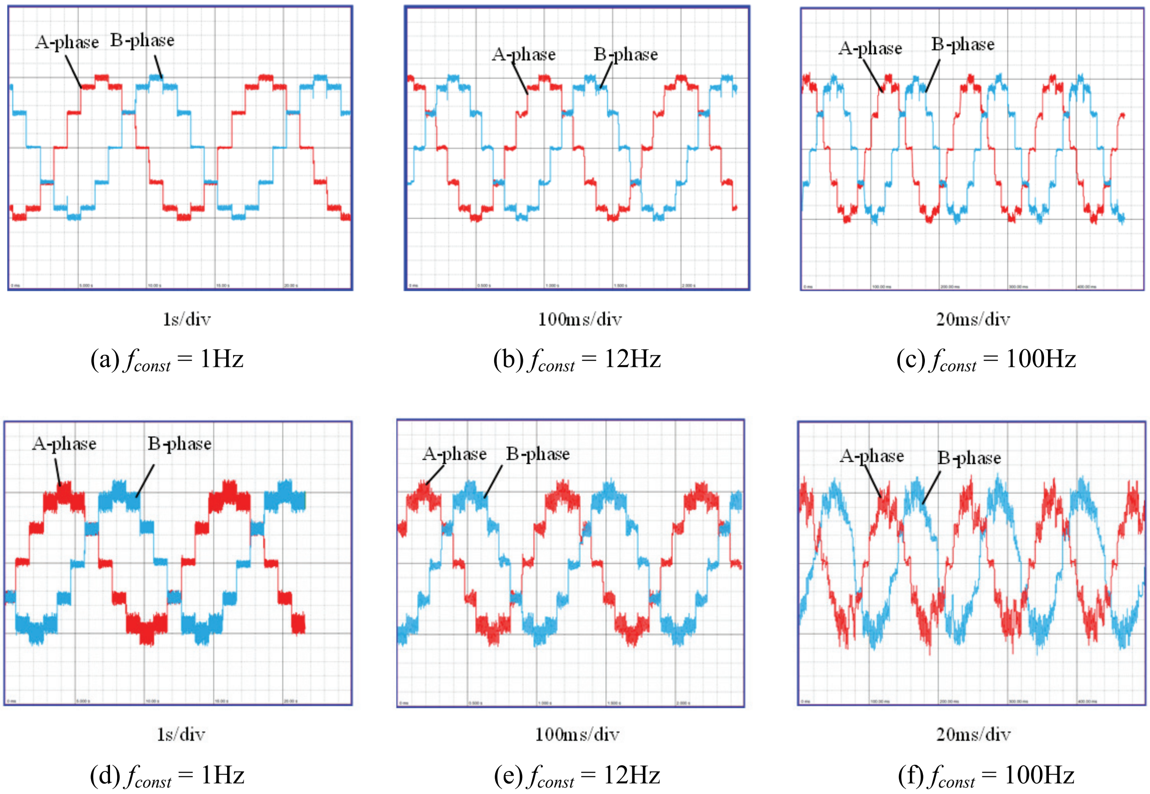

(a) f_{const} = 1Hz (b) f_{const} = 12Hz (c) f_{const} = 100Hz

(d) f_{const} = 1Hz (e) f_{const} = 12Hz (f) f_{const} = 100Hz

Fig. 8. Comparison of experiment waveform in different frequencies

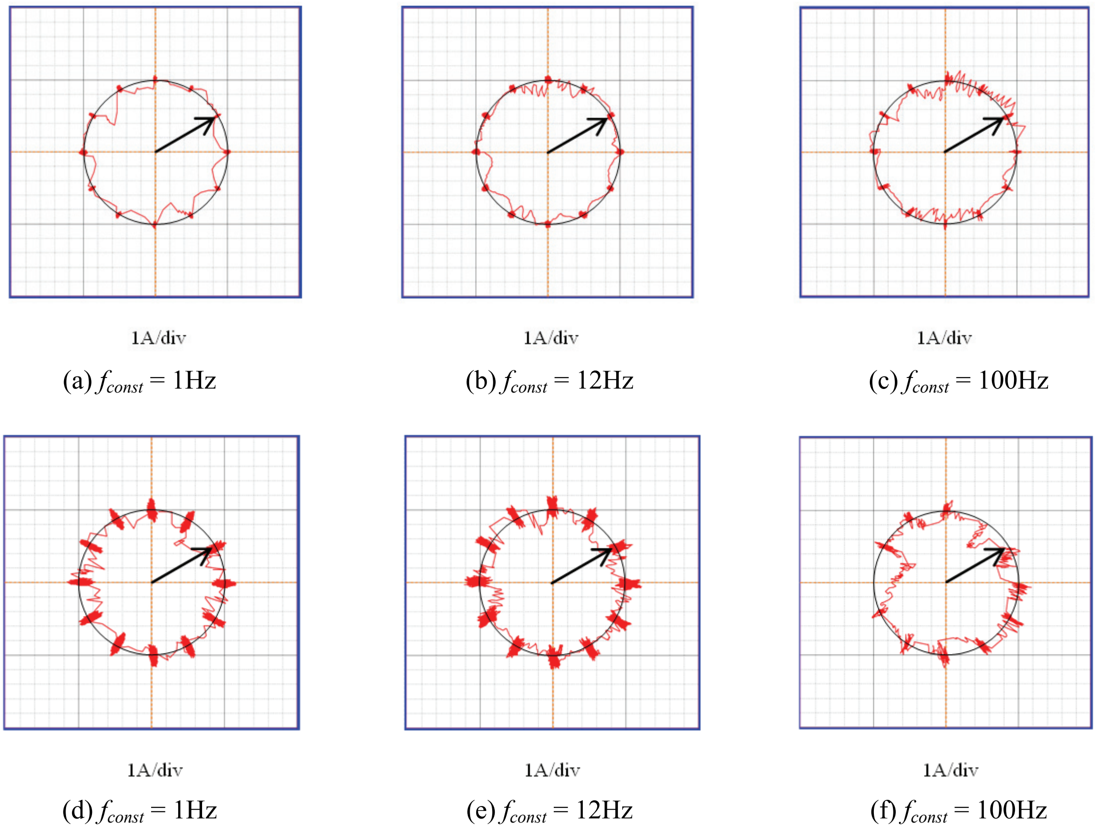

(a) f_{const} = 1Hz (b) f_{const} = 12Hz (c) f_{const} = 100Hz

(d) f_{const} = 1Hz (e) f_{const} = 12Hz (f) f_{const} = 100Hz

Fig. 9. Comparison of experiment current vector trajectory in different frequencies

in (d) is similar as (a), but the ripple of the current vector increases with the frequency in (e) and (f) and the transition process are not smooth enough.

4.4 Experiment results

The PMSM for experiment has been introduced in the previous section. The control system contains a DSP of TMS320F2407 chip as the core and the peripheral circuit of ADC, DAC and so on and the main part of power amplifier is an intelligent power module (IPM) PM15 RSH120. The other given conditions are the same as the simulation. The results of the control are observed by a waveform recorder that the actual current is measured by the clamp meter and the current vector is calculated in DSP and exported through DAC.

In Fig. 8, the top three (a), (b) and (c) are the actual current waveforms of A and B phase by the proposed method and the bottom three (d), (e) and (f) are by DCC. The oscillations of the current in the top three figures (less than 0.4A at the peak) are smaller than the bottom three (more than 1.6A at the peak). And when f_{const} = 100Hz, the current in (f) cannot track the given discrete sine waveform but in (c) the waveforms are satisfactory.

Fig. 9 will reflect the performance of current vector by the two methods. Drawing the reference circle that the radius is 5A, the tracking trajectory of the vector endpoint will be obviously shown in the figure. The top three (a), (b) and (c) are controlled by the proposed method that at the discrete point the vector can track the given with a little ripple. But the bottom three show the great tracking oscillations that in (d) and (e) the oscillations areas away from the discrete point are more than 8 times the size of the former, and in (f), the actual current vector cannot track the given point at all and the motor's running is not stable.

5. Conclusion

This paper has deduced the dynamic change of the stator current vector for PMSMs in α-β frame from the mathematics model. The dynamic change consists of three independent parts and can be simplify through Taylor series expansion. The predictive control has been put forward according to the dynamic change which is targeting the current vector, at the same time the interrelation of the current vector and the voltage vector in SVPWM has been deduced to testify the action of the space voltage vector and to improve the control method. The proposed method develops the control accuracy with the dynamic response of current vector and enhances the response speed by the direct control of the magnetic field targeting the current vector. Moreover, the method is easy to accomplish in α-β frame avoiding the coordinate transformation. At last, the performance of the proposed method has been verified by simulation and experiment compared with the DCC method.

Acknowledgements

This work was supported by the Hebei Natural Science Foundation Project (E2013202108), the Transformation of Important Scientific and Technological Achievements Project of Hebei (13041709Z) and the Hebei NDRC project (2013)

References

[1] Preindl M, Schaltz E. "Sensorless Model Predictive Direct Current Control Using Novel Second-Order PLL Observer for PMSM Drive Systems", IEEE Transactions on Industrial Electronics, vol. 58, no. 9, pp. 4087-4095, 2011

[2] Preindl M, Bolognani S. "Model Predictive Direct Speed Control with Finite Control Set of PMSM Drive Systems", IEEE Transactions on Power Electronics, vol. 28, no. 2, pp 1007-1015, 2013

[3] Sozer Y, Torrey D A, Mese, E. "Adaptive predictive current control technique for permanent magnet synchronous motors", IET Power Electronics, vol. 6, no. 1, pp. 9-19, 2013

[4] Joerg Weigold, Michael Braun. "Predictive Current Control Using Identification of Current Ripple", IEEE Transactions on Industrial Electronics, vol. 55, no. 12, December 2008

[5] Koichi Sakata, Hiroshi Fujimoto, Luca Peretti, et al. "Enhanced Speed and Current Control of PMSM Drives by Perfect Tracking Algorithms", The 2010 International Power Electronics Conference: 587-592

[6] NIU Li, YANG Ming, LIU Keshu, et al. "A Predictive Current Control Scheme for Permanent Magnet Synchronous Motors", Proceedings of the CSEE. 2012, 32(6): 131-137

[7] NIU Li, YANG Ming, WANG Geng, et al. "Research on the Robust Current Control Algorithm of Permanent Magnet Synchronous Motor Based on Deadbeat Control Principle", Proceedings of the CSEE. 2013, 33(15): 78-85

[8] YANG Nan-fang, LUO Guang-zhao, LIU Wei-guo. "Decoupling control of current loop for permanent magnet synchronous motor drives using error compensation", Electric Machines and Control. 2011, 15 (10): 50-54

[9] Wan Shanming, Wu Fang Huang Shenghua. "Analysis of digital current control loop for a PMSM", Journal of Huazhong University of Science and Technology (Nature Science Edition). 2007, 35(5): 48-51

[10] WANG Weihua, XIAO Xi. "A Current Control Method for Permanent Magnet Synchronous Motors with High Dynamic Performance", Proceedings of

the CSEE. 2013, 33(21): 117-123
[11] Yang Liyong, Zhang Yunlong, Chen Zhigang, et al. “On-Line Adaptive Control of PMSM Current-Loop Based on Parameter Identification”, Transactions of China Electrotechnical Society. 2012, 27(3): 86-91
[12] Wang Weihua, Xiao Xi, Ding Youshuang. “An Improved Predictive Current Control Method for Permanent Magnet Synchronous Motors”, Transact-ions of China Electrotechnical Society.2013, 28(3): 50-55
[13] Yan Zhi’an, Tang Ming, Yi Pinghu. “Space Vector Pulse Width Modulation Algorithm with Applications”, Journal of Xi’an Jiaotong University. 2006, 40(12): 1374-1377
[14] FANG Si-chen, LI Dan, ZHOU Bo, et al. “A Novel Algorithm of Space-vector PWM without Sector Calculation”, Proceedings of the CSEE. 2008, 28 (30): 35-40
[15] Sun Hexu. “AC stepping driving system”, Beijing: China Machine Press, 1996.7: 50-64
[16] Dong Yan, Sun Hexu, Bao Zhiyuan, et al. “Permanent Magnet Synchronous Motor Position Control System Based on Torque-Angle Control”, Transactions of China Electrotechnical Society. 2006, 21 (1): 86-91
[17] Dong Yan, Jing Kai, Sun Hexu, et al. “Discrete Current Control Strategy of Permanent Magnet Synchronous Motors”, Journal of Applied Mathematics. 2013(2013): 1-9
[18] V. Ambrožič, R. Fišer, and D. Nedeljković. “Direct current control-a new current regulation principle”, IEEE Transactions on Power Electronics [J], vol. 18, no. 1, pp. 495-503, 2003.

Hexu Sun He received the Ph.D. degree from Northeast University, Liaoning, China in 1993. He is currently a Professor of Hebei University of Technology and an IEEE Senior Member. His research interests are power electronics for utility application, electric motor, distributed power generation and the control for engineering system.

Kai Jing He is currently pursuing the Ph.D. degree in Hebei University of Technology, Tianjin, China. His research interests are power electronic and motor drives.

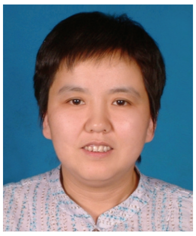

Yan Dong She received the Ph.D. degree from Hebei University of Technology, Tianjin, China in 2005. She is currently a Professor of Hebei University of Technology. Her research interests are electric transmission control and power electronics technology

Yi Zheng He received the Ph.D. degree from Hebei University of Technology, Tianjin, China in 2009. He is currently an Associate Professor of Hebei University of Technology. His research interests are Motion control and power electronics technology